




# Paleoclimate support for a persistent dry island effect in the Colombian Andes during the last 4700 years

The Holocene  
1–12  
© The Author(s) 2017  
Reprints and permissions:  
sagepub.co.uk/journalsPermissions.nav  
DOI: 10.1177/0959683617721324  
journals.sagepub.com/home/hol  


Broxton W Bird,<sup>1</sup> Owen Rudloff,<sup>1</sup> Jaime Escobar,<sup>2,3</sup>  
William P Gilhooly III,<sup>1</sup> Alex Correa-Metrio,<sup>4</sup>  
Maria Vélez<sup>5</sup> and Pratigya J Polissar<sup>6</sup>

## Abstract

We investigated middle- and late-Holocene hydroclimate patterns in the Colombian Andes using indicators of watershed erosion (lithic abundance), precipitation intensity (% silt), lake-level variability (organic carbon and nitrogen, % sand, and diatoms), and fire frequency (fossil charcoal) from a ~4700-year-long sediment archive from Laguna de Ubaque, a small sub-alpine lake on the eastern flank of the eastern Colombian Andes. Our results indicate reduced precipitation, low lake levels, and increased fire occurrence at Ubaque between 4700 and 3500 cal. yr BP (hereafter BP). Precipitation and lake levels increased abruptly while fire occurrence decreased between 3500 and 2100 BP, with the exception of a 300-year dry phase between 2800 and 2500 BP. Although wetter than the 4700–3500 BP interval, precipitation decreased, lake levels fell, and fire occurrence increased after 2100 BP, but with high-frequency variability. Comparison of the Ubaque results with other Colombian paleoclimate records (e.g. Lakes Fúquene and La Cocha) supports an antiphase pattern of precipitation between the high/interior Andes and frontal slope sites. This spatial pattern of variability is consistent with modern responses to the changes in terrestrial atmospheric convection associated with the so-called ‘dry island’ effect. Further comparison with paleoclimate records from Venezuela suggests that the millennial trend toward increasing frontal slope precipitation is consistent with orbitally induced increases in Andean atmospheric convection. Sub-orbital dry island-like hydroclimate variability suggests that other mechanisms that affect Northern Hemisphere convection may act to enhance or diminish this effect on centennial and shorter timescales.

## Keywords

Colombia, middle- and late-Holocene, paleoclimates, paleolimnology, sediment geochemistry, sedimentology

Received 9 January 2017; revised manuscript accepted 4 June 2017

## Introduction

Northern Hemisphere (NH) South American monsoon (SAM) variability is not as well characterized as its Southern Hemisphere (SH) counterpart because there are comparatively fewer paleo-hydroclimate records from the northern Andes (>0° latitude). Initially, the Cariaco Basin %Ti (titanium) record supported the idea that Holocene monsoon variability was antiphased between the hemispheres (Haug et al., 2001). Peak early Holocene NH monsoon intensity was attributed to a northerly position of the Inter-tropical Convergence Zone (ITCZ) in response to maximum NH insolation during the boreal summer, which reduced monsoonal intensity in the SH (Bird et al., 2011; Cruz et al., 2005; Haug et al., 2001; Thompson et al., 1995). Monsoonal precipitation subsequently diminished in the NH and increased in the SH as the ITCZ migrated southward through the Holocene in response to waning NH and increasing SH summer insolation, respectively. As an increasing number of paleoclimate records have become available from the NH Andes, however, a more complex pattern of Andean monsoon variability is emerging. Specifically, some regions in both Hemispheres (e.g. Venezuela, Peru, Bolivia, and northern Chile) experienced low lake levels during the middle-Holocene between 8000 and 2000 BP (calendar years before present; present = AD 1950), with wetter conditions and higher lake levels after ~2000 BP (Polissar et al., 2013). This suggests that at

least some portions of the northern and southern (<0° latitude) tropical Andes experienced similar and in-phase hydroclimate variability, which is counter to the ITCZ paradigm. Spatial patterns of NH Andean hydroclimate variability are complicated, however, with lake-level reconstructions from La Cocha (1.1°N, 77.2°W; González-Carranza et al., 2012) and Fúquene (05.5°N, 73.8°W; Vélez et al., 2006), both in Colombia, showing high lake levels from about 8000–3000 BP and lower lake levels to the

<sup>1</sup>Department of Earth Sciences, Indiana University–Purdue University, USA

<sup>2</sup>Universidad del Norte, Colombia

<sup>3</sup>Smithsonian Tropical Research Institute, Panama

<sup>4</sup>Departamento de Paleontología, Instituto de Geología, Universidad Nacional Autónoma de México, México

<sup>5</sup>Department of Geology, University of Regina, Canada

<sup>6</sup>Lamont-Doherty Earth Observatory, Columbia University, USA

## Corresponding author:

Broxton W Bird, Department of Earth Sciences, Indiana University–Purdue University, 723 W. Michigan St., SLI 118, Indianapolis, IN 46208, USA.

Email: bwbird@iupui.edu

present. While the Colombian lake-level trends appear to be opposite to those in other parts of the NH and SH Andes, contradicting the idea that Holocene Andean hydroclimate variability was interhemispherically coherent, the spatiotemporal responses of the Colombian Andes to insolation, ITCZ, and other forcings are not well characterized on paleoclimate timescales.

Precipitation in mountainous regions often displays complex spatial patterns associated with orographic controls on local atmospheric circulation (Garreaud et al., 2009; Roe, 2005). In Colombia, land-surface heating over the Andes modifies local atmospheric circulation during the boreal summer wet season (May–August), creating what has been described as a ‘dry island’ (the highland and interior Andes) in a ‘sea of rain’ (the frontal slopes; Snow, 1976). Strong convection induced by maximum mid-summer insolation enhances precipitation along frontal slopes, which strips moisture from the atmosphere and induces near-surface subsidence over the high and interior Andes (west of the Eastern Cordillera), creating a mid-summer precipitation minimum in these regions. Although changes in the strength of this so-called dry island effect have been suggested as an influence on the long-term altitudinal distribution of precipitation (Snow, 1976), instrumental and paleoclimate records are too short or lack sufficient temporal and spatial distributions to evaluate dry island variability on decadal to centennial timescales during the Holocene.

The stability of the dry island effect through time and its response to changes in climatic boundary conditions may be important for interpreting paleoclimate records from the Colombian Andes, including lake-level reconstructions, and their relationship with paleoclimate records from other parts of the northern and southern tropical Andes. For example, if convective atmospheric circulation over the Andes was reduced during the middle-Holocene as suggested by model simulations and paleoclimate studies (Cruz et al., 2009), we may expect Andean regions of Colombia to become wetter relative to other Andean regions, which could account for the apparently antiphased lake-level changes in the Colombian Andes compared with other regions in the NH and SH Andes (González-Carranza et al., 2012; Polissar et al., 2013).

Here, we use a well-dated lake sediment record from Laguna de Ubaque, a frontal slope lake in the eastern Colombian Andes, to investigate local hydroclimate variability during the middle- and late-Holocene. Past hydroclimatic conditions, including lake levels, watershed erosion, runoff energy, and fire occurrence, are reconstructed on decadal to multi-decadal timescales using a multi-proxy approach that integrates lithologic changes, grain size variability, measurements of the elemental abundances and isotopic composition of organic carbon and nitrogen, diatom composition, and charcoal abundances. Together with paleoclimate records from the eastern and central Colombian Andes, we investigate spatial relationships in hydroclimate variability between frontal slopes and the high/interior Andes during the last 4700 years to assess the stability and expression of the dry island effect. We further compare these results with paleoclimate records from Venezuela and Ecuador to investigate broader-scale hydroclimate patterns in NH South America.

## Study area

Laguna de Ubaque (hereafter Ubaque) is a small (0.093 km<sup>2</sup>), 14-m-deep sub-alpine lake located on the eastern flank of the Eastern Cordillera of the Colombian Andes at 2070 m a.s.l. (4.5°N, 73.9°W; Figures 1 and 2). Today, the lake is at least seasonally stratified with anoxic conditions below 8 m depth. Ubaque’s bathymetry is characterized by a flat profundal area that shallows gradually to the south and east and steeply to the west and north. The lake’s watershed measures 1.056 km<sup>2</sup> with headwalls that

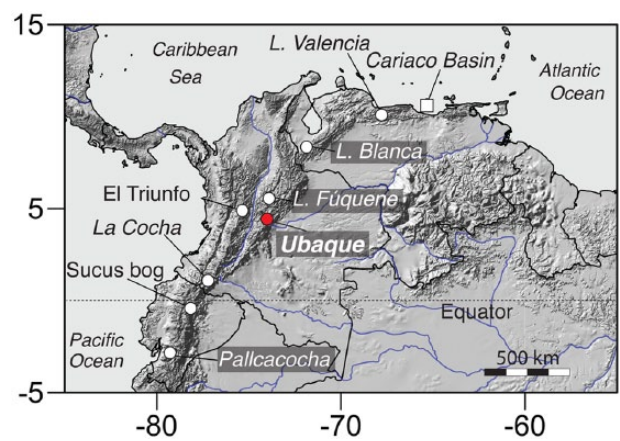


**Figure 1.** Map of northern South America showing the location of the study site (Ubaque, red circle) and other paleoclimate records discussed in the text (white circles).

reach 2600 m a.s.l. The local geology, as observed during field visits, comprises siliclastic sedimentary bedrock overlain by regolith, soils, and glacial deposits, including the terminal moraine damming the lake. These glacial deposits are likely pre-Holocene in age because the catchment’s headwall elevation is too low to have supported glaciations during the last ~10,000 years (Porter, 2000). Runoff from the watershed is focused by a small drainage on Ubaque’s northwestern shore before entering the lake. Deposition from fluvial inputs has created a delta in this region that extends into the lake (Figure 2). Although the lake level is high today, a small, manmade dam constructed within the last ~50 years at the low point in the lake’s moraine dam (eastern shore) regulates flow to control the lake’s level and minimize flooding of the houses that surround Ubaque (Figure 2). This suggests that if unmodified, the modern lake might be at least seasonally open, but also that periods of aridity could create closed hydrologic conditions.

The annual distribution of precipitation in the Colombian Andes is broadly characterized by two distinct spatial patterns that are expressed over the Andean frontal slopes and high and interior Andes (Snow, 1976). The interior region west of the Eastern Cordillera’s frontal slopes has two wet seasons – March, April, May (MAM) and September, October, November (SON) – and two dry seasons – June, July, August (JJA) and December, January, February (DJF; Figure 3). In contrast, the eastern slopes of the Eastern Cordillera feature a broad JJA precipitation maximum, even in sites within as little as 30 km of the high Andes. This spatial pattern has been attributed to the so-called dry island effect (Snow, 1976). Through this effect, summer heating results in large-scale convection over the Andes that advects lowland moisture up Andean frontal slopes, enhancing mid-summer precipitation in this region, but decreasing moisture delivery to the interior. Increased frontal slope precipitation and upper atmosphere divergence further cause non-precipitation producing air masses to descend over the high Andes, leading to elevated surface pressure, the formation of non-precipitation-bearing clouds, and a mid-summer precipitation minimum, creating a dry island (Snow, 1976). Two frontal slope weather stations close to Ubaque, Fomeque (4.3°N, 73.5°W, 1900 m a.s.l.) and Choachi (4.3°N, 73.6°W, 1950 m a.s.l.; Figure 3), are consistent with this climate pattern, showing peak precipitation between April and July, with elevated precipitation through October. This contrasts with the distribution of precipitation at nearby high Andean sites, such as near Bogota, which show reduced mid-summer precipitation characteristic of the dry island (Figure 3).

Wet-season moisture in the Eastern Cordillera is primarily derived from the tropical Atlantic (Gu and Zhang, 2001; Hastenrath, 2002; Poveda et al., 2005, 2006) and transported by easterly

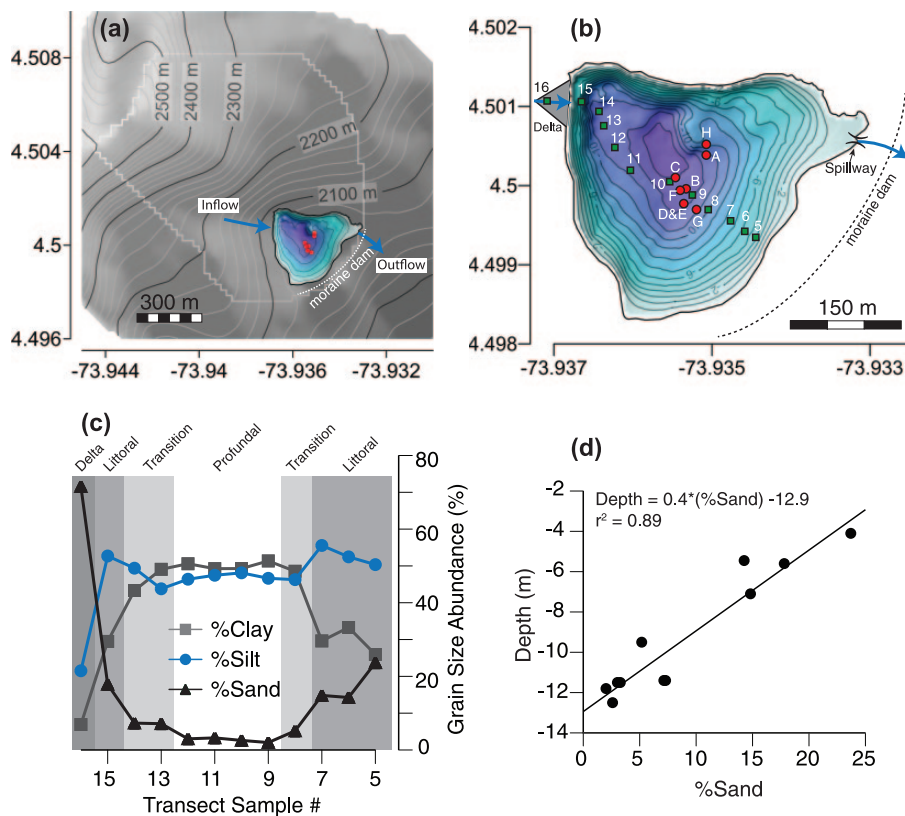


**Figure 2.** (a) Digital elevation map of the Ubaque watershed (outlined in gray) with inflows and outflows (labeled blue arrows) and the location of the moraine dam indicated (labeled white dashed line). (b) Bathymetric map of the Ubaque basin with the location from where sediment cores (red circles) and surface grab samples (green squares) were collected. The delta located on the lakes western shore is indicated with a large gray triangle. (c) Grain size abundance results from the surface sample transect. Littoral, transition, profundal, and delta regions are indicated. (d) Linear regression between water depth and % sand from the surface sample transect.

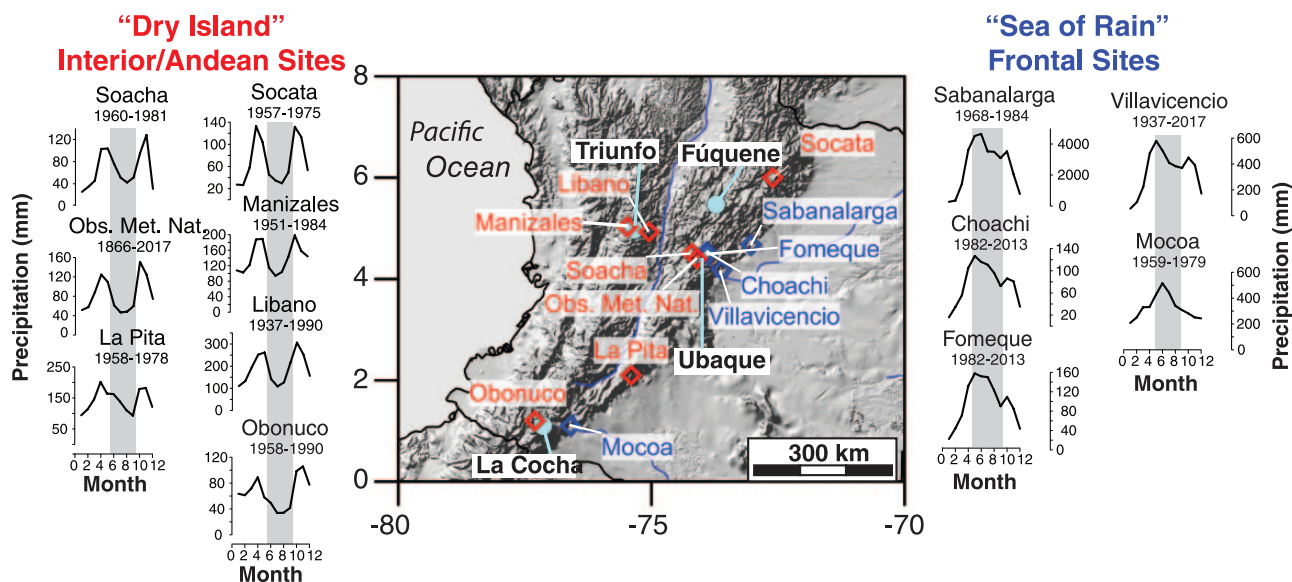


**Figure 3.** Map of the Colombian Andes showing the location of selected weather stations. Monthly average precipitation profiles for the individual weather stations are shown for interior/Andean sites (red open diamonds) and frontal slope sites (blue open diamonds). Data are from the Global Historical Climate Network with the data set duration shown below the station name. The gray vertical boxes indicate the mid-summer season from May through September. The location of Colombian paleoclimate records discussed in the text is also shown with light blue circles.

trade winds, which are at a maximum along the Eastern Cordillera at 850 mb (~1.5 km; Saylor et al., 2009). These trade winds converge over the Atlantic, which then follow an easterly path over South America. This trajectory oscillates between a zonal orientation during the boreal summer, channeling Atlantic moisture into northern South America, and a meridional orientation during the

boreal winter, channeling Atlantic moisture into the Amazon and away from northern South America. Amazonian moisture can also influence the Eastern Cordillera as a result of interactions between the Amazon-sourced South American low-level jet (Marengo et al., 2004; Poveda et al., 2005) and mesoscale convective systems that develop over the Amazon and Orinoco basins, which

**Table 1.** Ubaque radiocarbon ages.

Core	Drive	KCCAMS ID	Fxn modern	<sup>14</sup> C years BP	<sup>14</sup> C years BP ±	Calibrated age (cal. yr BP)	Mean composite depth (cm)	Thickness (cm)	Outlier probability	mg C <sup>a</sup>
D-13	1	132258	0.9400	500	120	520	43.5	0.7	0.01	0.015
D-13	1	132259	0.9260	620	40	600	81.5	1	0.25	0.044
D-13	2	132260	0.8553	1260	130	1170	115.5	1	0.01	0.015
D-13	3	132261	0.8137	1660	70	1570	163.5	1	0.01	0.027
D-13	3	132262	0.7812	1980	130	1940	203.5	1	0.01	0.015
D-13	6	132268	0.7332	2495	15	2580	299.5	0.1	0.01	
D-13	6	132264	0.6312	3700	100	4050	335.5	1	0.5	0.023
D-13	7	132265	0.6801	3095	30	3300	355.5	1	0.01	0.085
D-13	7	132266	0.6781	3120	15	3350	369.5	0.5	0.01	
F-13	7	132272	0.6053	4030	60	4520	417.5	1.5	0.01	0.038

<sup>a</sup>Provided for small samples.

lead to a JJA precipitation peak over the eastern piedmont of the Andes (Bonner, 1966; Garreaud et al., 2009; Maddox, 1980; Poveda et al., 2006; Velasco and Fritsch, 1987). This effect, however, diminishes northward. Isotopic analyses from a transect of sites from Bogota to the east shared an Atlantic signature, suggesting that modern precipitation at Ubaque is almost entirely Atlantic sourced (Saylor et al., 2009).

The temperature in the Colombian Andes exhibits little variability throughout the year because of its tropical setting (Poveda et al., 2007) and is strongly linked to elevation. Instrumental temperature records are not directly available from Ubaque, but a nearby weather station in Tibacuy, Colombia (4.4°N, 74.5°W; 1550 m a.s.l.), which is at a similar elevation, exhibits a largely uniform annual temperature profile. Temperatures here averaged 19.2°C and varied by a maximum of 0.8°C between 1952 and 1980 (Peterson and Vose, 1997).

At interannual scales, the El Niño–Southern Oscillation (ENSO) is the primary driver of tropical South American hydroclimate (Poveda et al., 2005). In Colombia, El Niño events are typically associated with reduced precipitation and increased temperature, whereas precipitation increases and temperatures are cooler during La Niña events (Garreaud et al., 2009; Poveda et al., 2005, 2011). Decadal to centennial SAM precipitation variability is not well understood because long-term instrumental data are limited. Pacific decadal variability (PDV), however, has been identified as an influence on Colombian and northern South American climate in ways similar to ENSO. Positive PDV conditions result in diminished precipitation and increased temperatures across Colombia, and negative PDV conditions result in increased precipitation and decreased temperatures (Evans et al., 2001). The strength of ENSO events is also enhanced when they are of the same sign as the PDV phase (Andreoli and Kayano, 2005; Kayano and Andreoli, 2007).

## Materials and methods

### Sediment collection

Seven sediment cores were collected from Ubaque in July 2013 (Figure 2b). The sediment–water interface was collected in three surface cores using a modified piston corer. Four long cores were collected with a modified Livingstone piston corer (Wright Jr et al., 1984). Individual 1-m drives were collected sequentially with 30 cm overlap between drives to ensure complete sediment recovery. A 445-cm-long composite core was constructed by visually matching distinct stratigraphic units between cores. Refusal was reached at 445 cm because of stiff sediments. Eleven surface sediment samples were collected using an Ekman grab sampler along a northwest–southeast transect in 2015 (Figure 2b).

All samples were transported to the Indiana University–Purdue University Indianapolis (IUPUI) Paleoclimatology and Sedimentology Laboratory and stored at 4°C.

### Sediment core processing, dry bulk density, and loss-on-ignition

Sediment cores were split, photographed, described, and volumetrically sub-sampled (1 cm<sup>3</sup>) at 2-cm intervals for dry bulk density and loss-on-ignition (LOI) analysis. These samples were weighed wet, dried for 24 h at 60°C, and reweighed to determine dry bulk density ( $\rho_{\text{dry}}$ ; g cm<sup>-3</sup>). Total organic matter (% TOM) and total carbonate (% TC) abundances were determined by LOI after combustion at 550°C (4 h) and 1000°C (2 h), respectively (modified from Boyle, 2001; Heiri et al., 2001). The bulk density and LOI results are described in the supplemental materials (Figure S1, available online).

### Dating and age control

Age control for the Ubaque record was established by accelerator mass spectrometry radiocarbon analysis AMS <sup>14</sup>C of 10 samples at the University of California, Irvine, Keck AMS Laboratory (Table 1). Charcoal and macroscopic terrestrial organic material >63 µm were picked from a wet sieve after a brief disaggregation in a 7% hydrogen peroxide solution. Samples were physically cleaned and chemically pretreated following acid–base–acid protocols. Ages are reported as the median probability and 1σ error after calibration to calendar years before present using the Bayesian age modeling software package Bacon (Blaauw and Christen, 2011) and the IntCal13 data set (Reimer et al., 2013). All dates referred to in the text are in cal. yr BP unless otherwise noted. Dating of the upper most sediment was attempted with <sup>210</sup>Pb and <sup>137</sup>Cs, but concentrations of these radionuclides were below detection limits.

### Lithics and grain size

Approximately 1 g of wet sediment was collected at 1 cm intervals from the composite core ( $n = 445$  samples) for grain size analysis. Samples were dried for 24 h at 60°C, weighed, and then treated with 30%–35% H<sub>2</sub>O<sub>2</sub> to remove OM (Gray et al., 2010). Biogenic silica was removed from each sample with a 20-mL 1 N NaOH digestion (6 h at 60°C). Carbonates were digested with an acid-washing procedure (20 mL of 1 N HCl for 1 h). Samples were then freeze-dried and reweighed to determine lithic abundance (% lithics). Grain size measurements were made using a Malvern Mastersizer 2000 with reported values being the average of three replicate measurements. Grain size results were parsed into 49 particle size diameter bins between 0.2 and 2000 µm.

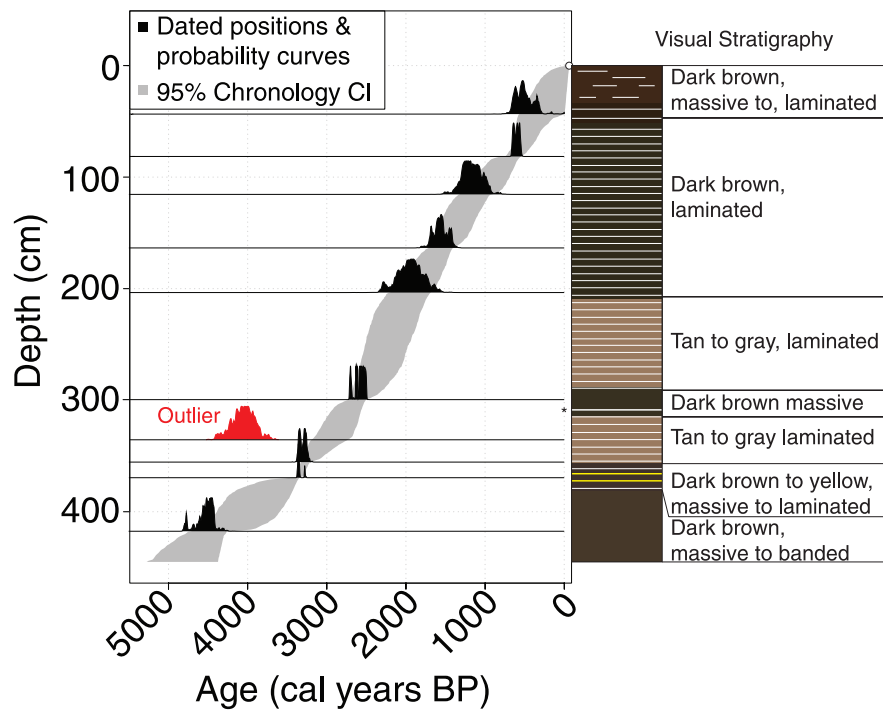


**Figure 4.** Age–depth model constructed with Bacon for the Ubaque core showing the location and probability curves of dated positions (black curves and associated horizontal lines) and the 95% confidence interval (CI) range of the age model (gray shading). One outlier is indicated with the red curve. Visual stratigraphy of the Ubaque composite core is also shown with brief descriptions of the lithostratigraphic units. The asterisk marks the location of suspected volcanic tephra layers.

#### Elemental abundance and isotopic composition of organic carbon and total nitrogen

The elemental abundance and isotopic composition of organic carbon ( $C_{\text{org}}$  and  $\delta^{13}C_{\text{org}}$ ) and total nitrogen (N and  $\delta^{15}N$ ) were determined by combustion with an elemental analyzer (Costech Analytical) coupled with a Delta V Plus stable isotope ratio mass spectrometer (Thermo Scientific). Approximately 6 mg of freeze-dried sample was weighed into tin capsules for isotopic analysis for both acidified ( $\delta^{13}C$ ) and un-acidified ( $\delta^{15}N$ ) replicates. The elemental standard acetanilide (C = 71.09%, and N = 10.36%) was used to correct elemental abundances based on the peak area response of the TCD detector. Carbon ( $\delta^{13}C$ ) and nitrogen ( $\delta^{15}N$ ) isotopic data are reported in the supplemental materials (Figure S1, available online).

#### Charcoal

Charcoal concentrations were determined for 86 samples (0.5 cm<sup>3</sup>) of the Ubaque composite sediment core. Sediment samples were deflocculated using hot  $Na_4P_2O_7$  (10%) for more than 20 minutes, and charcoal particles were separated by hand under 40 $\times$  magnification (Clark, 1988). A digital photograph of the recovered particles from each sample was analyzed using ImageJ (Rasband et al., 2005) to determine the area covered by each piece of charcoal. Charcoal area was then standardized by volume analyzed and expressed as concentration (mm<sup>2</sup> cm<sup>-3</sup>).

#### Diatoms

Sediment samples were collected at ~5 cm intervals ( $n = 100$ ) from the Ubaque composite core for diatom analysis. Each sample was treated for 24 h at room temperature with 30 mL of  $H_2O_2$  (30%), and 10 mL of HCl was added to the sample and later washed with distilled water. Permanent slides were prepared with Naphrax, and a minimum of 350 diatoms were counted at 100 $\times$  magnification. Diatom identification and ecology were described following literature (Gaiser and Johansen, 2000; Krammer et al.,

1986; Krammer and Lange-Bertalot, 1991; Lange-Bertalot and Krammer, 2000; Moro and Fürstenberger, 1997; Patrick and Reiner, 1966; Torgan and Biancamano, 1991).

## Results

The original data presented here are archived online at the NOAA Paleoclimatology Database (<https://www.ncdc.noaa.gov/paleo/study/2275>).

#### Modern grain size distributions

Surface sediment grab samples were used to characterize grain size distributions in littoral (samples 5, 6, 7, and 15), transitional (samples 8, 13, and 14), and profundal regions (samples 9–12) at Ubaque (Figure 2b and c). Sand abundances were highly correlated with water depth ( $r = 0.95$ ,  $p < 0.001$ ), showing the highest abundances in littoral regions (17.6%) and lower abundances in transitional (6.5%) profundal zones (2.7%). Clay was also highly correlated with depth ( $-0.94$ ,  $p < 0.001$ ), with high abundances in the profundal zone (50.1%) and lower abundances in intermediate (47.0%) and littoral (29.6%) zones. Silt showed no correlation with water depth and was instead evenly distributed across the littoral (52.8%), transitional (46.5%), and profundal zones (47.2%).

#### Stratigraphy

The Ubaque sediment core was divided into seven sections based on visible stratigraphy (Figure 4). Between 445 and 390 cm, Ubaque sediments are largely massive and organic rich, but with occasional banding. A transition to finely laminated sediments occurs between 390 and 360 cm, with millimeter-scale laminae alternating in color between yellow-green and dark brown. Between 360 and 315 cm, sediments become more finely laminated and finer grained with an overall light gray to brown color. From 315 to 285 cm, the sediments abruptly become massive and darker brown, but with some banding. This section also contains two notable gritty white layers at 311 cm comprising angular

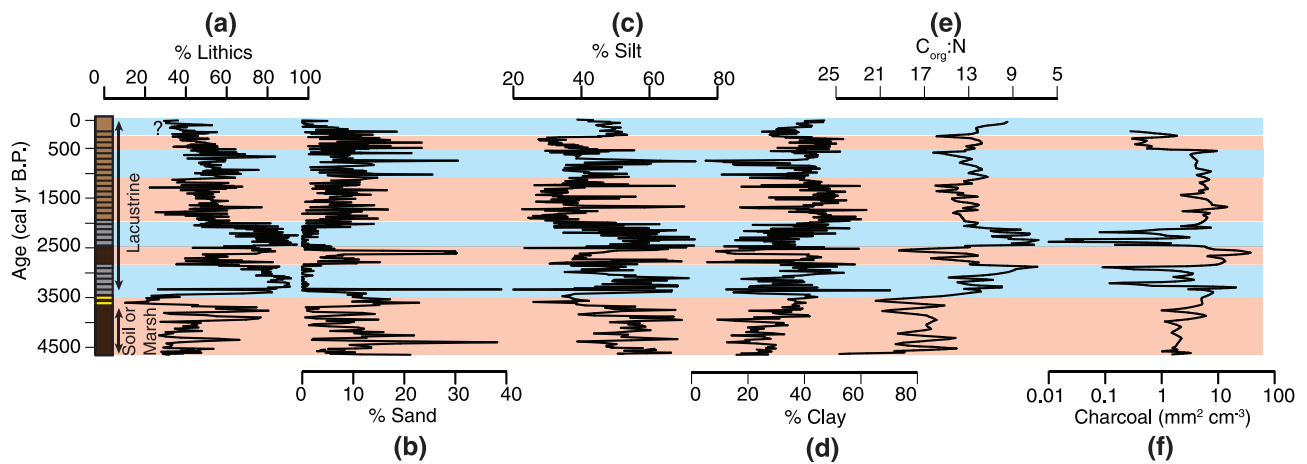


**Figure 5.** Results from the Ubaque sediment record for (a) % lithics with a simplified stratigraphic profile at left, (b) % sand, (c) % silt, (d) % clay, (e)  $C_{org}:N$  (reversed axis), and (f) charcoal concentration ( $mm^2 cm^{-3}$ ). Colored horizontal boxes represent periods of drier (red) and wetter (blue) conditions. Dry conditions during the earliest part of the record are primarily inferred from high  $C_{org}:N$ , whereas the most recent wet phase is based primarily on decreased  $C_{org}:N$  and increased % silt. The question mark at the top of the lithics plot indicates the divergent trend in lithics compared with other hydroclimate indicators that suggest wetter conditions after 300 BP.

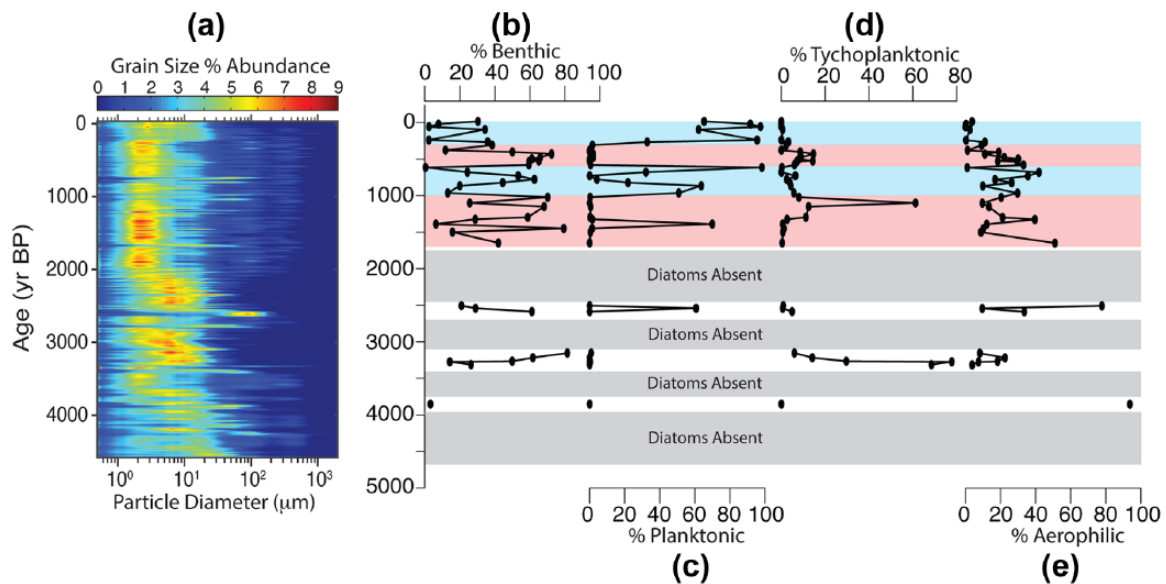


**Figure 6.** (a) Shaded histogram showing temporal variations in abundance of grain sizes in the Ubaque sediment record. Abundance variations in (b) benthic, (c) planktonic, (d) tychoplanktonic, and (e) aerophilic diatoms in the Ubaque sediment record.

glass fragments consistent with volcanic tephra. Between 285 and 215 cm, the sediments revert abruptly to light gray-brown laminae. From 215 to 51 cm, laminae are observed, but the sediments darken to a brown color. Above 51 cm, laminae are intermittent, becoming indiscernible above 35 cm.

### Chronology

Nine of the 10 AMS  $^{14}C$  ages are in stratigraphic order with only one sample (KCCAMS# 132264) returning an older than expected age (Figure 4). Given that it is bracketed by ages in chronostratigraphic order, we assigned this sample a 50% probability of being an outlier during the age model construction. The age model generally shows steady accumulation with slightly higher rates of accumulation between 3200 and 2000 BP and slightly lower rates of accumulation from the bottom of the core from 4650 to 3200 BP and after 2000 BP.

### Lithics and grain size

Lithic abundances (% lithics, hereafter lithics) exhibited considerable variability, with a maximum of 95%, a minimum of 10%,

and a mean of 57% during the record (Figure 5). The average lithics were low between 4650 and 3450 BP, but with increasing variability and average values (mean = 40.3%). Lithics were generally high between 3450 and 2050 BP (3450–2850 BP mean = 78.4%; 2600–2050 BP mean = 79.6%), except for the period between 2820 and 2600 BP when they fell to an average of 54.9%. After 2050 BP, lithics varied about a mean of 49.9% with lower values between 2050 and 1050 and 600 BP to the present and high values between 1050 and 600 BP. Clay and silt are the two most abundant grain size fractions, together accounting for 92.5% of the lithic fraction, and demonstrate a strong anti-correlation throughout the record ( $r = -0.84$ ) as expected from the sum-to-one constraint. Clay abundance varied between 15% and 80%, with a mean of 46% while the silt fraction ranged between 18% and 73%, with a mean of 46% (Figures 5 and 6). Grain size results for silt and clay are described in terms of silt, with the understanding that the opposite trends occurred in clay abundances.

From 4650 to 3700 BP, silt varied around a mean of 54.7% (Figure 5). At 3700 BP, silt declined sharply, averaging 36% between 3700 and 3440 BP. Silt then increased to an average of 58.5% between 3440 and 2760 BP, after which silt decreased to

39% until ~2600 BP. After ~2600 BP, silt increased sharply to an average of 63% between ~2600 and 2000 BP. From 2000 to present, silt was generally lower than before 2000 BP, but with considerable variability. Periods with elevated silt are noted between 1050 and 730, 620 and 500, and after 280 BP with low silt during the intervening periods.

Sand is the least abundant sediment constituent, generally comprising less than 20% of the lithics with an average of 6.5% and a range from 0% to 38% (Figure 5). The sand record displays considerable variability that shares some similarities with silt and clay, but also contains distinct variability. Sand was generally high, but variable between 4650 and 3370 BP, after which point it decreased to less than 0.5% between 3300 and 2830 BP. After 2830 BP, sand increased to an average of 8% between 2800 and 2500 BP with peak values reaching ~30% at 2600 BP. Sand then abruptly decreased again between 2500 and 2080 BP, after which point it increased and maintained an average of approximately 8%. After ~300 BP, sand shows a decreasing trend to modern values averaging ~2%.

#### Organic-carbon-to-nitrogen ratio ( $C_{org}:N$ )

Down-core organic-carbon-to-nitrogen ratio ( $C_{org}:N$ ) measurements were divided into three intervals (Figure 5). From 4650 to 3500 BP,  $C_{org}:N$  was at a maximum, averaging 17.5 with a maximum of 24.7. Between 3500 and 2100 BP,  $C_{org}:N$  exhibited considerable variability with two lows, each reaching 6.7 between 3400 and 2860 and 2480 and 2100 BP that were separated by a peak of 19.7 between 2800 and 2500 BP. After 2100 BP,  $C_{org}:N$  values were intermediate (~13), with minor fluctuations.

#### Diatoms

Modern diatoms recovered from the surface samples are composed mainly of benthic *Achnantheidium minutissimum*, found in the shallow platform of the lake, and *Achnantheidium lanceolatum* found predominantly in the pelagic region, between 7 and 12 m along with Tycho planktonic *Fragilaria nanana*. Benthic *Encyonopsis cf krammeri*, *Encyonema silesiacum*, and *Nitzschia amphibia* dominate in the mouth of the inlet. Fossil diatom preservation and/or occurrence were generally poor with only 39% samples being suitable for analysis (Figure 6; Figure S2, available online). Preservation was especially poor before 1660 BP with only 9 of 61 samples containing diatoms (14.75%) with abundant broken valves showing mechanical damage. Diatoms were abundant at 3920, from 3320 to 3180 BP, 2570 to 2490 BP, and after 1660 BP. From 3920 to 2530 BP, *Synedra ulna*, *F. nanana*, *Aulacoseira ambigua*, *Navicula radiosa*, and *Craticula* sp. peak with values around 70%. After 1660 BP, valve preservation improved, but was still sporadic with ~30% of samples lacking diatoms. *A. ambigua* became dominant (20%–98%) after 1660 BP, but with other species also present, including *Craticula* sp. (25%–30%), *Staurisirella pinnata* (two peaks of 20% and 87%), *Eunotia minor* (3%–33%), and *Gomphonema* sp. (2–54%). Aerophil diatoms, mainly *Luticola mutica*, *Hantzschia amphioxys*, *Diademsis confervacea*, and *Orthoseira* sp., were present at 3920 (93%), 2500 (78%), and between 1425 and 300 BP (22%). After 300 BP, the assemblage was dominated by *A. ambigua* (20%–98%), but *N. amphibia* also increased (20% max) as did *Cyclotella meneghiniana* and *Achnantheidium* sp. (40% and 28%, respectively).

#### Charcoal

Charcoal concentrations at Ubaque ranged from  $9 \times 10^{-3}$  to  $39 \text{ mm}^2 \text{ cm}^{-3}$ , with a mean and standard deviation of 4.3 and  $5.4 \text{ mm}^2 \text{ cm}^{-3}$ , respectively. Between 4650 and 3900 BP, charcoal concentrations were low, remaining below  $3 \text{ mm}^2 \text{ cm}^{-3}$ , and increasing to

$21 \text{ mm}^2 \text{ cm}^{-3}$  between 3900 and 3300 BP (Figure 5). Charcoal concentrations decreased to  $1.5 \text{ mm}^2 \text{ cm}^{-3}$  between 3250 and 2870 BP, after which they reached maximum values, increasing to  $13 \text{ mm}^2 \text{ cm}^{-3}$  at 2770 BP and then to  $39 \text{ mm}^2 \text{ cm}^{-3}$  at 2630 BP. After 2630 BP, charcoal concentrations decreased to below 3 between 2460 and 2140 BP, after which they again increased to an average of  $5 \text{ mm}^2 \text{ cm}^{-3}$  between 2140 and 520. From 520 to 140 BP, charcoal concentrations remained below  $3 \text{ mm}^2 \text{ cm}^{-3}$ , representing the minima throughout the record.

## Discussion

### Sediment grain size

In lacustrine settings, grain size can reflect a variety of transport and depositional processes including changes in the runoff energy transporting sediment to the lake and/or the depositional energy at the core site (Bird et al., 2014; Bird and Kirby, 2006; Conroy et al., 2008; Håkanson, 1982; Shuman et al., 2009). To better interpret down-core sedimentological changes, we first connect grain size distributions to modern depositional environments (i.e. littoral, transitional, and profundal zones) using the surface sediment grab samples (Figure 2b). The surface sample grain size data demonstrate that sand abundances vary as a function of water depth (Figure 6). This is consistent with previous studies that demonstrate littoral regions are dominated by coarse sediment fractions in response to rapid settling of coarser grains once runoff loses competence as it enters a standing body of water and redistribution through near-shore wave action (Dearing, 1997; Digerfeldt, 1986; Newby et al., 2000; Shuman, 2003; Shuman et al., 2001).

At Ubaque, we suggest that periods with little or no sand content represent lake high stands, which increased the distance between the core site and the littoral zone, thereby reducing the delivery of sand to more profundal reaches. Conversely, high sand content indicates periods when the littoral zone encroached toward the core site in the profundal zone, delivering more sand to the deeper parts of the lake. As a semi-quantitative estimate of past lake levels at Ubaque, we derived a transfer function between % sand and depth utilizing the modern depth–sand relationship constrained by the surface sample transect (Figure 2d; delta sample #15 not included;  $\text{depth} = 0.4 \times (\% \text{ sand}) - 12.9$ ;  $r^2 = 0.89$ ).

Elevated sand from 4650 to 3400 BP suggests that lake levels during this period were likely lower than those captured by the modern sediment samples (Figure 5). As a result, the modern relationship between sand and lake depth likely is not analogous and so the transfer function does not apply for this time interval.

After 3400 BP, sand decreased rapidly with minima between 3360 and 2830 and 2530 and 2060 BP, suggesting high lake stands equivalent to modern conditions (~13 m). These lake high stands are separated by a ~300-year low stand between 2820 and 2550 BP, during which lake levels fell to as low as 2 m. Elevated sand percentages after 2060 BP suggest average lake levels around 9 m, with slightly elevated lake levels from 2100 to 1100 and after 200 BP and slightly lower lake levels between 1100 and 200 BP.

Like sand, clay abundances vary strongly with depth in the modern surface samples (Figure 2). Despite this modern correlation with depth, down-core measurements of clay are not significantly correlated with sand abundances ( $r = -0.075$ ,  $p = 0.12$ ; Figure 5). Instead, clay is strongly antiphased with silt ( $r = -0.84$ ,  $p < 0.001$ ). This indicates that clay abundances in the down-core record were controlled by variations in the abundance of silt, not lake depth. As such, we interpret down-core changes in clay and silt as indicators of the intensity/energy of runoff such that higher intensity runoff would increase the amount of silt in the water column relative to clay, and vice versa (Bird et al., 2016).

This interpretation is less clear for the period prior to ~3500 BP because of the likelihood that grain size distributions in a shallow, marsh-like system that possibly desiccated at times may not reflect the same processes as those acting in deeper, permanent lake systems. Wave action and bioturbation as a result of low water levels and possible pedogenesis (indicated by massive sedimentology and high C:N and OM) may additionally homogenize silt layers deposited during discrete events, thereby increasing silt's apparent overall abundance. For these reasons, silt results prior to ~3500 BP should be interpreted cautiously and we refrain from interpreting silt as an indicator of runoff energy during this period.

After ~3500 BP, silt abundances show two maxima from 3440 to 2760 and ~2600 to 2000 BP, suggesting high-energy runoff during these periods of intense precipitation and deep-lake conditions as indicated by finely laminated sediments. The intervening silt minimum between 2760 and 2600 BP coincides with a return to massive sediments, suggesting reduced runoff intensity during this interval when precipitation was reduced and lake levels fell sharply. Lower average silt after 2000 BP suggests less intense runoff at a time when lake levels were lower, but still deep enough to support potentially anoxic hypolimnetic conditions as suggested by the preservation of fine laminations. Increased silt between 1050 and 730, 620 and 500, and after 280 BP, however, suggests periods of greater runoff intensity within this drier mean state. Low silt abundances between ~2000 and 1050 BP and 500 and 280 BP suggest intervening periods of low-intensity runoff.

#### Lithic abundances

The abundance of lithic material deposited in lake systems reflects the relative contribution of clastic material to the sediment fraction. At Ubaque, the lake's surficial unconsolidated glacial deposits and steep watershed topography provide ample sediment and potential energy for runoff to erode material during the wet season and transport it directly to the lake. We interpret increased lithics to represent periods when precipitation was greater and watershed erosion was enhanced, and vice versa. From 4690 to 3500 BP, average lithics was lower than at any other period in the record (mean = 41%), but with a positive trend and increasing variability, suggesting increasing precipitation with punctuated periods of watershed erosion (Figure 5). The increase to maximum lithics between 3500 and 2100 BP coincides with the transition to laminated, organic poor sediments, reflecting a marked increase in watershed erosion that we attribute to increased precipitation. This period was briefly interrupted by a ~200-year dry interval between 2800 and 2600 BP, during which massive, organic-rich sediments were deposited. Reduced lithics after 2100 BP suggests decreased erosion, but with slightly increased erosion between 1050 and 600 BP that was followed by decreasing, but variable, erosion to the present.

#### $C_{org}:N$ ratio

Atomic carbon and nitrogen ratios are used to distinguish the relative contribution of terrestrial ( $C_{org}:N > 15$ ) and aquatic ( $C_{org}:N < 15$ ) OM to the lake sediment (Meyers and Ishiwatari, 1993). We suggest that low  $C_{org}:N$  values reflect expanded lake surface areas during high stands, which both limited terrestrial OM deposition to the littoral zone and increased in-lake productivity and deposition of aquatic OM in the profundal zone. The opposite is proposed for low lake stands.

Within the above interpretive framework, the  $C_{org}:N$  data indicate that the Ubaque record is broadly characterized by two distinct end-member depositional settings. Between 4650 and 3500 BP,  $C_{org}:N$  ratios averaged 17.7 with a maximum of 24.7, and % OM averaged 50%, indicating a significant contribution of terrestrial OM that suggests extremely low lake levels and/

or marsh-like conditions during this time (Figure 5; Figure S1, available online). Sediments during this interval were also massive with high sand abundances, suggesting a shallow, oxygenated water column and sediment bioturbation/mixing. After 3500 BP, decreasing  $C_{org}:N$  values were accompanied by a transition to finely laminated sediments and low sand abundances, indicating a shift to persistent deep-lake conditions. Variability in  $C_{org}:N$  after 3500 BP, however, suggests fluctuating lake levels with especially deep-lake conditions from 3400 to 2860 (11.4) and 2470 to 2100 BP (9.0). Separating these intervals, a pronounced low stand occurred between 2800 and 2500 BP (14.4). These inferred lake-level fluctuations are consistent with lithologic indicators of high stands (i.e. laminations) and low stands (i.e. massive sediments indicating bioturbation). Although somewhat elevated  $C_{org}:N$  values after 2100 BP (13.1) suggest lower lake levels, the presence of laminated sediment indicates that lake levels were deep enough to support a stratified water column with anoxic bottom waters that precluded bioturbation. Variability in  $C_{org}:N$  values, however, suggests lake levels still fluctuated during this time, but with less amplitude than before 2100 BP. Relative low stands are suggested by  $C_{org}:N$  peaks between 1400 and 1240 (~16) and at 600 (16.2) and 260 BP (15.9). Relative high stands are suggested by  $C_{org}:N$  lows between 1150 and 850 (~12.1), 530–300 (~11.8), and from 160 BP to the present (~11.3).

#### Diatoms

Diatom valve preservation is discontinuous in the record to 1660 BP (Figure 6). Between 4690 and ~3300 BP, the general lack of diatoms is attributed to the persistence of marsh-like conditions at Ubaque and/or periods of sub-aerial exposure that limited diatom preservation in the sediment archive. Between 3300 and 1660 BP, we interpret the low abundance of diatoms to have resulted from high water column turbidity, which inhibited photosynthesis, as a result of increased lithic influx to the lake when precipitation was as a maximum (e.g. Bird et al., 2014). A rapid increase in lake level occurred after ~3330 BP is indicated by increased abundances of Tychoplanktonic species *S. ulna* and *F. nanana*, which are found today in the pelagic area of the lake. Benthic species, *Craticula* sp. and *N. radiosa*, and shallow planktic, *A. ambigua*, indicate the presence of a developed littoral zone at this time. Although not very common at Ubaque today, this species lives in the transitional zone between 5 and 7 m depth. Fluctuating, but diminished, precipitation intensity after 1660 BP lead to stable lake conditions and the development of a stable littoral area, which promoted the long-term proliferation and preservation of diatom communities. The general dominance of shallow planktic and benthic communities after 1660 BP supports persistent, but somewhat lower lake levels during the late-Holocene. Notably, increases in *A. ambigua*, *N. amphibia*, and *F. pinnata* between 1070 and 610 BP and after 300 BP indicates an increase in the nutrient content of the lake. This agrees well with  $C_{org}:N$  and silt and sand, which suggest wetter conditions during these times (despite low lithic abundance for the post 300 BP period), which either brought more nutrients to the water or re-suspended them from the littoral zone.

#### Charcoal as a proxy for watershed moisture conditions

Charcoal concentration in lacustrine settings reflects both local and regional fire frequencies, which in turn reflect hydroclimatic conditions as well as fuel availability (Clark, 1988). Higher charcoal concentrations indicate increased biomass burning and vice versa. Here, total charcoal trends largely track inferred changes in precipitation and lake levels (Figure 5). During times when indicators suggest wetter conditions and high lake stands, for example, the dual precipitation peaks between 3500 and 2000 BP,



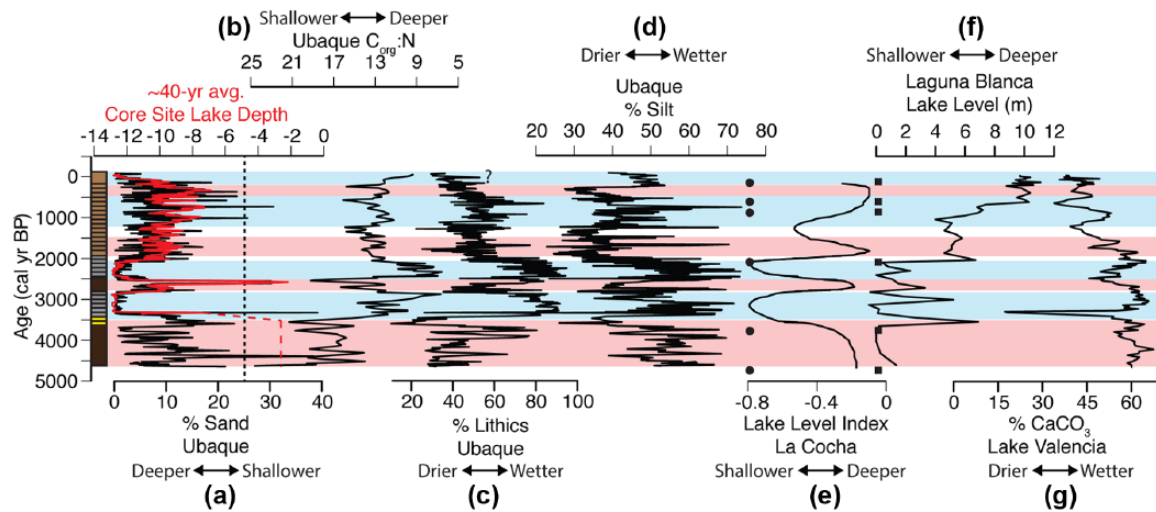


**Figure 7.** Correlations of regional hydroclimate records. (a) % Sand (black line) is overlaid with ~40-year average lake levels estimated using the modern lake depth–% sand relationship shown in Figure 2 (red line). Qualitative lake levels are represented with a dashed red line for the part of the Ubaque record when marsh-like/terrestrial conditions are inferred from the  $C_{org}:N$  data. The vertical black dashed line indicates the minimum lake depth represented by the modern calibration samples. (b)  $C_{org}:N$  as a proxy for lake levels at Ubaque. (c) % Lithics at Ubaque as a proxy for watershed erosion related to wetter (higher lithics) or drier (lower lithics) conditions. The question mark indicates the divergent trend in lithics compared with other hydroclimate indicators that suggest wetter conditions after 300 BP. (d) % Silt at Ubaque as a proxy for the energy of runoff from the lake's watershed whereby increased silt reflects wetter conditions and lower silt reflects drier conditions. (e) La Cocha, CO, diatom-derived lake-level index. Black circles indicate the position of  $^{14}C$  ages. (f) Laguna Blanca, VZ, lake-level reconstruction. Black squares indicate the position of  $^{14}C$  ages. (g) Lake Valencia, VZ, %  $CaCO_3$  as an indicator of wetter (higher %  $CaCO_3$ ) or drier (lower %  $CaCO_3$ ) conditions. The gray arrow between Ubaque % silt and the La Cocha lake-level reconstruction indicates what we interpret to be correlative wet and dry periods, respectively.

charcoal abundances were at a minimum. Conversely, when hydroclimate indicators suggest drier conditions, charcoal concentrations increase, for example, the period of drought centered around ~2700 and again after 2100 BP. The antiphased relationship between charcoal and moisture availability suggests that although dry episodes were recurrent, conditions were never sufficiently dry so as to suppress fire because of a lack of biomass to burn. Notably, charcoal abundances decreased after approximately 550 BP when other hydroclimate indicators suggest dry conditions. One possibility is that cooling during the Little Ice Age contributed to reduced fire occurrence (e.g. Polissar et al., 2006) despite evidence for drier conditions at Ubaque.

#### Lake-level and hydroclimate interpretation of the Ubaque record

The multi-proxy Ubaque record suggests a series of significant hydroclimate changes over the past ~4700 years. In general, dry conditions characterized by periods of low lake levels, marsh-like conditions, and possibly intervals of terrestrialization predominated from ~4650 to 3500 BP. After 3500 BP, precipitation and lake levels increased, with two periods at 3500–2800 and 2500–2100 BP being the wettest intervals during the past ~5000 years. These wet intervals were interrupted by a ~300-year-long drought, during which lake levels fell to as low as 2 m. After ~2100 BP, the climate became drier, but was still wetter than before 3500 BP, with shallower, but persistent deep-lake conditions. Within this period, wet phases occurred at ~1100–550 and after ~300 BP with intervening dry periods.

#### A persistent dry island effect in the Colombian Andes

Although there are few Colombian paleo-hydroclimate records, those available show climatically similar results when compared with the Ubaque records that are consistent with modern Colombian hydroclimate processes. The most proximal record to Ubaque is from El Triunfo mire, which is located in the central Colombian Andes at 3800 m a.s.l. about 160 km west of Ubaque (4.98°N,

75.33°W; Vélez et al., in preparation). Although both El Triunfo and Ubaque were relatively dry between ~4700 and 3500, they demonstrate consistent opposite hydroclimate trends after 3500 BP. Increased precipitation at Ubaque from 3500 to 2100 BP coincided with continued low water levels at El Triunfo. After ~2300 BP, water levels increased at El Triunfo but decreased at Ubaque. Although the results from Triunfo are relatively low resolution, their antiphased relationship with Ubaque is consistent with that predicted between interior and/or high-elevation sites and those on the frontal slopes (i.e. Ubaque).

This antiphased relationship between frontal slopes and interior sites is additionally supported by the relationships between Ubaque and a diatom-based lake-level reconstruction from La Cocha in southern Colombia (González-Carranza et al., 2012). The La Cocha lake-level curve, which is constrained by six  $^{14}C$  ages during the past 4800 years, exhibits a consistent antiphased relationship with Ubaque over the last ~4700 years (Figure 7). Reduced precipitation at Ubaque from ~4700 to 3500 BP, for example, corresponds to high lake levels and precipitation at La Cocha. The alternating wet–dry–wet period at Ubaque from 3500 to 2100 BP similarly corresponds to a dry–wet–dry sequence at La Cocha (i.e. low–high–low lake levels). Drier conditions at Ubaque during the last 2100 years were generally wetter at La Cocha, but with variability that continued to be antiphased with Ubaque, supporting a continued hydroclimate antiphasing relationship between Andean and frontal slope sites through the late-Holocene.

The La Cocha trends are largely similar to first-order lake-level changes documented at Lake Fúquene on the western side of the eastern Colombian Andes at 2540 m a.s.l. (Vélez et al., 2006). Minimum Holocene lake levels at Fúquene occurred at 4230–1770 BP with generally wetter conditions before and after this time. The timing of the Fúquene low stand is similar to increasing precipitation and lake levels at Ubaque at 3500–2100 BP, further supporting an antiphased hydroclimate relationship between frontal slopes and high/interior Andean sites.

The antiphased relationship between Ubaque, as a frontal slope site on eastern Colombian Andes, with interior/high-altitude

sites represented by La Cocha, Fúquene, and El Triunfo is consistent with modern-day seasonal variations in the distribution of precipitation across the Colombian Andes related to the dry island effect (Snow, 1976). This suggests that the dry island effect is not only important on seasonal timescales during the modern instrumental period, but also an important component of multi-decadal to multi-centennial-scale Colombian hydroclimate during at least the last ~4700 years.

The modern dry island effect observed on seasonal timescales is attributed to (1) strong convection during the mid-summer insolation maximum that enhances rainout along the Andean flanks, which depletes air masses of moisture prior to their reaching higher elevations and interior locations over the Colombian Andes, and (2) upper atmosphere divergence that causes non-precipitation air masses to descend over the high Andes, elevating surface pressure and causing the formation of non-precipitation bearing clouds.

The elevational distribution and geographical location of the Ubaque (2067 m a.s.l.; eastern Colombian Andes frontal slope), El Triunfo (3800 m a.s.l.; central Colombian Andes), and La Cocha (2780 m a.s.l.; interior southern Colombian Andes) records and their opposing hydroclimate trends is consistent with the dry island phenomenon and suggests that pluvial phases at Ubaque represent periods of strong convection and rainout with correspondingly drier conditions at high elevation and interior sites such as El Triunfo and La Cocha as a result of air mass moisture depletion during transport and atmospheric subsidence.

#### *Comparison with northern South America hydroclimate records*

When considered in the context of other regional paleoclimate records from northern South America, the Ubaque record suggests complex, but explainable, hydroclimate variability during the middle- and late-Holocene (Figure 7). Comparison between Ubaque and a lake-level reconstruction from Laguna Blanca in the Venezuelan Merida Andes (8.3°N, 71.8°W; 1615 m a.s.l.), whose age model consists of six <sup>14</sup>C ages over the last 4800 years, shows that both sites were drier from ~4700 to 3500 BP (Polissar et al., 2013). Lake levels at Blanca began to increase by ~3500 BP, but with considerable variability, whereas Ubaque became abruptly wetter at ~3500 BP. Lake levels at Blanca subsequently increased stepwise at 2100 and ~600 BP, while lake levels and precipitation decreased at Ubaque at 2100 BP and subsequently varied about a mean until 600 BP, after which time wetter conditions are indicated by silt and diatom results. Still, conditions at Ubaque were wetter after 2100 BP than before 3500 BP.

Despite some differences in centennial-scale hydroclimate variability at Ubaque and Blanca, the millennial-scale trend toward generally wetter conditions at Blanca and Ubaque during the late-Holocene (after ~3500 BP) relative to the middle-Holocene (before ~3500 BP) is similar. Given that hydroclimate variability at Ubaque is reflective of the intensity of convective precipitation, generally wetter late-Holocene conditions at Ubaque and Blanca may suggest increasing convective precipitation at these sites after ~3500 BP. That Ubaque became much wetter than Blanca between ~3500 and 2100 BP and then dried slightly after 2100 BP, whereas Blanca shows a steady increase in lake levels, may reflect their different geographic settings, whereby Ubaque is a true frontal slope site influenced by the dry island effect and Blanca is intermediate between frontal slope and high Andean environments as it is at relatively low elevation (1615 m), but situated on the down-wind side of the Andes from the dominant moisture transport direction. Regardless, the basic pattern of increased late-Holocene Andean convection suggested by the Ubaque and Blanca records is consistent with orbital configurations that would have increased overall convection across the Andes (Cruz et al., 2009).

Comparison of Ubaque with a carbonate abundance record (interpreted as relative lake level) from Lake Valencia, Venezuela (10.2°N, 67.7°W; 410 m a.s.l.), shows that wet conditions at Valencia at ~5000–3500 BP coincided with low lake levels and reduced precipitation at Ubaque and Blanca (Curtis et al., 1999). It is possible that as a site located longitudinally in the middle of northern South America, Valencia was affected earlier by the westward migration of terrestrial atmospheric convection over tropical South America (e.g. Cruz et al., 2009), while sites located further west in the Venezuelan (Blanca) and Colombian (Ubaque) Andes responded later (~3500 BP). Additional records from Venezuela and Colombia that span different elevations are needed, however, to better test this idea.

After ~3500 BP, wet and dry periods were broadly in phase at Ubaque and Valencia. Both records also show a drying trend after ~2000, although Valencia continues to become drier while Ubaque varies about a generally drier mean state (Figure 7). The shift to drier conditions at lower elevation sites (Ubaque and Valencia) and wetter conditions at altitude (Blanca, La Cocha, and Triunfo) after ~2000 BP may suggest weakened convective atmospheric circulation that reduced rainout on frontal slopes and at lower elevation, but increased moisture delivery to higher elevation sites. Although the dry island effect has not been explicitly described in Venezuela, the Venezuelan Andes do experience a mid-summer precipitation minimum, similar to the Colombian Andes, which has been linked, in part, to topographic influences and strengthened upper level easterly winds (Pulwarty et al., 1998). The region surrounding Valencia, likewise, experiences a mid-summer precipitation maximum, similar to Colombian frontal slope sites. It is possible, therefore, that the antiphased high- and low-elevation hydroclimate trends on millennial timescales could reflect broadly similar dry island-like variability on paleoclimate timescales in northern South America, but with some modification from regional factors.

Because reductions in atmospheric convective activity after ~2100 BP suggested by the Ubaque and other records occurred during an orbital configuration that would have increased overall convection across the Andes relative to the middle-Holocene (e.g. Cruz et al., 2009), other influences on convective activity must be considered. One possibility is that the onset of modern ENSO variability at ~2000 BP (Moy et al., 2002; Rodbell et al., 1999) and a more persistent El Niño-like mean state in the tropical Pacific (Koutavas et al., 2006), likely in response to orbital forcing (Emile-Geay et al., 2007), could have increased synoptic-scale atmospheric subsidence that somewhat suppressed convection over northern tropical South America. This, in turn, would weaken the dry island effect, decreasing frontal slope precipitation and increasing moisture delivery to higher elevation and interior sites.

## **Conclusion**

The Ubaque sediment record reflects variations in local hydroclimate on the frontal slopes of the eastern Colombian Andes during the last ~4700 years. Comparison with interior/high-elevation paleoclimate records from the eastern and central Colombian Andes indicates that the so-called dry island effect, whereby increased atmospheric convection enhances precipitation over frontal slope regions while reducing it at interior and high-altitude sites, and vice versa, has been an integral component of Colombian hydroclimate variability since at least the middle-Holocene. Reduced convection over the Colombian Andes is suggested for the middle-Holocene until ~3500 BP when Ubaque was relatively dry, but high Andean sites in Colombia were wet with generally high lake levels (e.g. Lakes Fúquene and La Cocha). Increasing precipitation and higher lake levels at Ubaque after ~3500 BP with peak pluvial conditions between ~3500 and 2100 BP and corresponding lake level and precipitation decreases at high/

interior Andean sites indicate strong convective activity and an enhanced dry island effect. After 2100 BP, reduced precipitation and lower lake levels at Ubaque and correspondingly higher lake levels at interior/high Andean sites indicate weakening late-Holocene convection (although it was still stronger than during the middle-Holocene).

The millennial-scale trend at Ubaque from a drier middle-Holocene (before ~3500 BP) to a wetter late-Holocene (after ~3500 BP) is consistent with an increase in orbitally forced convective activity over western South America. Despite generally increasing convective precipitation over western South America from the middle- to late-Holocene, slightly reduced precipitation at Ubaque and increasingly wet conditions at high Andean sites after ~2100 BP suggests some suppression of atmospheric convection that reduced precipitation at frontal sites and increased it at interior/Andean sites. This shift may be due, in part, to the onset of modern ENSO variability and a more persistent El Niño-like sea surface temperature pattern in the tropical Pacific during the late-Holocene, which served to increase atmospheric subsidence over northern South America, despite more westerly located convection in response to orbital forcing.

While intriguing, additional high-resolution Holocene hydroclimate records are needed from the Colombian Andes (frontal and high Andean sites) to test the idea that the dry island effect was an important mode of Andean climate variability through the Holocene. The persistence of dry island-like variability could potentially reconcile differences between hydroclimate records from the Colombian Andes and those from other parts of the Andes, which show different Holocene trends. For example, higher lake levels and increased precipitation in the Colombian Andes (e.g. La Cocha) during the middle-Holocene (8000–3000 BP) may reflect a dry island response to reduced Andean convection during this time, which manifested as drier conditions in other parts of the Andes as indicated by low lake levels in the Venezuelan and Peruvian/Chilean Andes (e.g. Lake Titicaca). One implication for a persistent dry island effect is that a common driver of interhemispheric tropical Andean hydroclimate variability, that is, changes in large-scale atmospheric convection, could be invoked to explain the generally synchronous, but complex, Holocene hydroclimate changes observed in the NH and SH Andes. That abrupt and sustained Holocene hydroclimate variability in the NH and SH Andes does not closely resemble the gradual changes in the position of the ITCZ inferred from the Cariaco Basin, or the oxygen and hydrogen isotope records of monsoon variability from many Andean lakes, speleothems, and ice cores, may suggest that local Andean climate was more, or additionally, sensitive to large-scale Andean atmospheric convection. The close correspondence between the Cariaco Basin ITCZ record and South American isotope-based monsoon records could additionally suggest that ITCZ variability was more influential in the core SAM region over the Amazon Basin. To test these ideas, additional high-resolution paleoclimate records of local Andean hydroclimate variability (at high and low elevations) are needed from the NH and SH Andes. For Colombia specifically, understanding how changes in Andean convection may affect the spatial distribution of precipitation in mountain regions, where the majority of water retention systems are located, is important for assessing the stability of water resources.

### Acknowledgements

Co-first authors: B.W.B. and O.R.

### Funding

J.E. and M.V. were partially supported by a grant from the Inter-American Institute for Global Change Research (IAI) CRN3038, which is supported by the US National Science Foundation (grant GEO-1128040). B.W.B. was partially supported by grants from

the US National Science Foundation (EAR 1445649) and Indiana University–Purdue University, Indianapolis, IN (RSFG & IDF).

### References

- Andreoli RV and Kayano MT (2005) ENSO-related rainfall anomalies in South America and associated circulation features during warm and cold Pacific decadal oscillation regimes. *International Journal of Climatology* 25: 2017–2030.
- Bird BW, Abbott MB, Rodbell DT et al. (2011) Holocene tropical South American hydroclimate variability revealed from a decadal resolved lake sediment  $\delta^{18}\text{O}$  record. *Earth and Planetary Science Letters* 310: 192–202.
- Bird BW and Kirby ME (2006) An alpine lacustrine record of early Holocene North American Monsoon dynamics from Dry Lake, southern California (USA). *Journal of Paleolimnology* 35: 179–192.
- Bird BW, Lei Y, Perello M et al. (2016) Late-Holocene Indian summer monsoon variability revealed from a 3,300-year-long lake sediment record from Nir'pa Co, southeastern Tibet. *The Holocene*. Epub ahead of print 28 September. DOI: 10.1177/0959683616670220.
- Bird BW, Polissar PJ, Lei Y et al. (2014) A Tibetan lake sediment record of Holocene Indian summer monsoon variability. *Earth and Planetary Science Letters* 399: 92–102.
- Blaauw M and Christen JA (2011) Flexible paleoclimate age-depth models using an autoregressive gamma process. *Bayesian Analysis* 6: 457–474.
- Bonner WD (1966) Case study of thunderstorm activity in relation to the low-level jet. *Monthly Weather Review* 94: 167–178.
- Boyle JF (2001) Inorganic geochemical methods in paleolimnology. In: Last WM and Smol JP (eds) *Tracking Environmental Change Using Lake Sediments*. Dordrecht: Kluwer Academic Publishers, pp. 83–141.
- Clark JS (1988) Particle motion and the theory of charcoal analysis: Source area, transport, deposition, and sampling. *Quaternary Research* 30: 67–80.
- Conroy JL, Overpeck JT, Cole JE et al. (2008) Holocene changes in eastern tropical Pacific climate inferred from a Galápagos lake sediment record. *Quaternary Science Reviews* 27: 1166–1180.
- Cruz F, Burns SJ, Karmann I et al. (2005) Insolation-driven changes in atmospheric circulation over the past 116,000 years in subtropical Brazil. *Nature* 434: 63–66.
- Cruz FW, Vuille M, Burns SJ et al. (2009) Orbitally driven east-west antiphasing of South American precipitation. *Nature Geoscience* 2: 210–214.
- Curtis JH, Brenner M and Hodell DA (1999) Climate change in the Lake Valencia Basin, Venezuela, approximately 12,500 yr BP to present. *The Holocene* 9: 609–619.
- Dearing J (1997) Sedimentary indicators of lake-level changes in the humid temperate zone: A critical review. *Journal of Paleolimnology* 18: 1–14.
- Digerfeldt G (1986) Studies on past lake-level fluctuations. In: Berglund BE (ed.) *Handbook of Holocene Palaeoecology and Palaeohydrology*. New York: Wiley, pp. 127–143.
- Emile-Geay J, Cane MA, Seager R et al. (2007) El Niño as a mediator of the solar influence on climate. *Paleoceanography* 22: PA3210.
- Evans MN, Cane MA, Schrag DP et al. (2001) Support for tropically-driven Pacific decadal variability based on paleoproxy evidence. *Geophysical Research Letters* 28: 3689–3692.
- Gaiser EE and Johansen J (2000) Freshwater diatoms from Carolina Bays and other isolated wetlands on the Atlantic coastal plain of South Carolina, USA, with descriptions of seven taxa new to science. *Diatom Research* 15: 75–130.
- Garreaud RD, Vuille M, Compagnucci R et al. (2009) Present-day South American climate. *Palaeogeography, Palaeoclimatology, Palaeoecology* 281: 180–195.

- González-Carranza Z, Hooghiemstra H and Vélez MI (2012) Major altitudinal shifts in Andean vegetation on the Amazonian flank show temporary loss of biota in the Holocene. *The Holocene* 22: 1227–1241.
- Gray AB, Pasternack GB and Watson EB (2010) Hydrogen peroxide treatment effects on the particle size distribution of alluvial and marsh sediments. *The Holocene* 20: 293–301.
- Gu G and Zhang C (2001) A spectrum analysis of synoptic-scale disturbances in the ITCZ. *Journal of Climate* 14: 2725–2739.
- Håkanson L (1982) Bottom dynamics in lakes. *Hydrobiologia* 91: 9–22.
- Hastenrath S (2002) The intertropical convergence zone of the eastern Pacific revisited. *International Journal of Climatology* 22: 347–356.
- Haug GH, Hughen K, Sigman DM et al. (2001) Southward migration of the intertropical convergence zone through the Holocene. *Science* 293: 1304–1308.
- Heiri O, Lotter AF and Lemcke G (2001) Loss on ignition as a method for estimating organic and carbonate content in sediments: Reproducibility and comparability of results. *Journal of Paleolimnology* 25: 101–110.
- Kayano MT and Andreoli RV (2007) Relations of South American summer rainfall interannual variations with the Pacific Decadal Oscillation. *International Journal of Climatology* 27: 531–540.
- Koutavas A, Olive GC and Lynch-Stieglitz J (2006) Mid-Holocene El Niño–Southern Oscillation (ENSO) attenuation revealed by individual foraminifera in eastern tropical Pacific sediments. *Geology* 34: 993–996.
- Krammer K and Lange-Bertalot H (1991) *Süsswasserflora von Mitteleuropa. Bacillariophyceae, vol 1 part 4. Achnanthesaceae*. Jena-Stuttgart: Gustav Fisher Verlag.
- Krammer K, Lange-Bertalot H, Krammer K et al. (1986) *Bd. 2: Bacillariophyceae*. Stuttgart: Fischer Verlag.
- Krammer K and Lange-Bertalot H (2000) *Süsswasserflora von Mitteleuropa. Bacillariophyceae, vol 1 part 3. Centrales, Fragilariaceae, Eunotiaceae*. Jena-Stuttgart: Gustav Fisher Verlag.
- Maddox RA (1980) Mesoscale convective complexes. *Bulletin of the American Meteorological Society* 61: 1374–1387.
- Marengo JA, Liebmann B, Vera CS et al. (2004) Low-frequency variability of the SALLJ. *Clivar Exchanges* 9: 26–27.
- Meyers PA and Ishiwatari R (1993) Lacustrine organic geochemistry—An overview of indicators of organic matter sources and diagenesis in lake sediments. *Organic Geochemistry* 20: 867–900.
- Moro RS and Fürstenberger CB (1997) *Catálogo dos principais parâmetros ecológicos de diatomáceas não-marinhas*. Parana, Brazil: Ed. Universidade Estadual de Ponta Grossa.
- Moy CM, Seltzer GO, Rodbell DT et al. (2002) Variability of El Niño/Southern Oscillation at millennial timescales during the Holocene epoch. *Nature* 420: 162–165.
- Newby PE, Killoran P, Waldorf MR et al. (2000.) 14,000 years of sediment, vegetation, and water-level changes at the Makepeace Cedar Swamp, southeastern Massachusetts. *Quaternary Research* 53: 352–368.
- Patrick R and Reiner C (1966) *The Diatoms of the United States Exclusive of Alaska and Hawaii*. Philadelphia, PA: Academy of Natural Sciences.
- Peterson TC and Vose RS (1997) An overview of the Global Historical Climatology Network temperature database. *Bulletin of the American Meteorological Society* 78: 2837–2849.
- Polissar PJ, Abbott MB, Wolfe AP et al. (2006) Solar modulation of Little Ice Age climate in the tropical Andes. *Proceedings of the National Academy of Sciences* 103: 8937–8942.
- Polissar PJ, Abbott MB, Wolfe AP et al. (2013) Synchronous interhemispheric Holocene climate trends in the tropical Andes. *Proceedings of the National Academy of Sciences* 110: 14551–14556.
- Porter SC (2000) Snowline depression in the tropics during the Last Glaciation. *Quaternary Science Reviews* 20: 1067–1091.
- Poveda G, Álvarez DM and Rueda ÓA (2011) Hydro-climatic variability over the Andes of Colombia associated with ENSO: A review of climatic processes and their impact on one of the Earth's most important biodiversity hotspots. *Climate Dynamics* 36: 2233–2249.
- Poveda G, Waylen PR and Pulwarty RS (2006) Annual and interannual variability of the present climate in northern South America and southern Mesoamerica. *Palaeogeography, Palaeoclimatology, Palaeoecology* 234: 3–27.
- Poveda G, Mesa OJ, Salazar LF et al. (2005) The diurnal cycle of precipitation in the tropical Andes of Colombia. *Monthly Weather Review* 133: 228–240.
- Poveda G, Vélez JI, Mesa OJ et al. (2007) Linking long-term water balances and statistical scaling to estimate river flows along the drainage network of Colombia. *Journal of Hydrologic Engineering* 12: 4–13.
- Pulwarty R, Barry R, Hurst C et al. (1998) Precipitation in the Venezuelan Andes in the context of regional climate. *Meteorology and Atmospheric Physics* 67: 217–237.
- Rasband MN, Tayler J, Kaga Y et al. (2005) CNP is required for maintenance of axon–glia interactions at nodes of Ranvier in the CNS. *GLIA* 50: 86–90.
- Reimer PJ, Bard E, Bayliss A et al. (2013) IntCal13 and Marine13 radiocarbon age calibration curves 0–50,000 years cal BP. *Radiocarbon* 55(4): 1869–1887.
- Rodbell DT, Seltzer GO, Anderson DM et al. (1999) An ~15,000-year record of El Niño driven alluviation in southwestern Ecuador. *Science* 283: 516–520.
- Roe GH (2005) Orographic precipitation. *Annual Review of Earth and Planetary Sciences* 33: 645–671.
- Saylor JE, Mora A, Horton BK et al. (2009) Controls on the isotopic composition of surface water and precipitation in the Northern Andes, Colombian Eastern Cordillera. *Geochimica et Cosmochimica Acta* 73: 6999–7018.
- Shuman BN (2003) Controls on loss-on-ignition variation in cores from two shallow lakes in the northeastern United States. *Journal of Paleolimnology* 30: 371–385.
- Shuman BN, Newby P and Donnelly JP (2009) Abrupt climate change as an important agent of ecological change in the Northeast US throughout the past 15,000 years. *Quaternary Science Reviews* 28: 1693–1709.
- Shuman BN, Bravo J, Kaye J et al. (2001) Late Quaternary water-level variations and vegetation history at Crooked Pond, southeastern Massachusetts. *Quaternary Research* 56: 401–410.
- Snow J (1976) The climate of northern South America: Colombia. In: Schwedtfeger W (ed.) *Climates of South and Central America*. Amsterdam: Elsevier Scientific Publishing Company, pp. 358–379.
- Thompson LG, Mosley-Thompson E, Davis ME et al. (1995) Late Glacial Stage and Holocene Tropical Ice Core Records from Huascarán, Peru. *Science* 269: 46–50.
- Torgan LC and Biancamano MI (1991) *Catálogo das diatomáceas ('Bacillariophyceae') referidas para o Estado do Rio Grande do Sul, Brasil, no período de 1973 a 1990*. Caderno de Pesquisa, serie Botanica. Faculdades Integradas de Santa Cruz do Sul 1: 5–196.
- Velasco I and Fritsch JM (1987) Mesoscale convective complexes in the Americas. *Journal of Geophysical Research: Atmospheres (1984–2012)* 92: 9591–9613.
- Vélez M, Hooghiemstra H, Metcalfe S et al. (2006) Late Glacial and Holocene environmental and climatic changes from a limnological transect through Colombia, northern South America. *Palaeogeography, Palaeoclimatology, Palaeoecology* 234: 81–96.
- Wright H Jr, Mann D and Glaser P (1984) Piston corers for peat and lake sediments. *Ecology* 65: 657–659.